isvr Institute of Sound and Vibration Research

The Effects of Track Non-Linearity on Wheel/Rail Impact

T.X. Wu and D.J. Thompson

ISVR Technical Memorandum 912

June 2003

University of Southampton

SCIENTIFIC PUBLICATIONS BY THE ISVR

Technical Reports are published to promote timely dissemination of research results by ISVR personnel. This medium permits more detailed presentation than is usually acceptable for scientific journals. Responsibility for both the content and any opinions expressed rests entirely with the author(s).

Technical Memoranda are produced to enable the early or preliminary release of information by ISVR personnel where such release is deemed to the appropriate. Information contained in these memoranda may be incomplete, or form part of a continuing programme; this should be borne in mind when using or quoting from these documents.

Contract Reports are produced to record the results of scientific work carried out for sponsors, under contract. The ISVR treats these reports as confidential to sponsors and does not make them available for general circulation. Individual sponsors may, however, authorize subsequent release of the material.

UNIVERSITY OF SOUTHAMPTON

INSTITUTE OF SOUND AND VIBRATION RESEARCH

DYNAMICS GROUP

The Effects of Track Non-Linearity on Wheel/Rail Impact

by

T.X. Wu and D.J. Thompson

ISVR Technical Memorandum No: 912

June 2003

Authorised for issue by
Professor M.J. Brennan
Group Chairman

Abstract

Wheel/track impact due to rail joints or wheel flats has been studied over many years. The railway track is usually assumed to be linear in order to simplify the track model, although the rail pad and ballast are actually non-linear. This may cause incorrect results to some extent in some circumstances, as the pad and ballast stiffness varies with load. In this paper wheel/track impact is studied using a non-linear track model. The rail is represented by an FE model and is supported by a non-linear track foundation. Wheel/track impacts are simulated at different train speeds and three types of rail pad, soft, medium and stiff, are used in the simulations. It is shown that the impact forces rise dramatically when the stiff rail pads are used. On the other hand, using soft pads can reduce impact forces significantly. Compared with the results from the linear track model, both the impact force and the track vibration level are shown to be noticeably higher from the non-linear track than those from the linear track. It is therefore concluded that linear track models are not appropriate for wheel/track impact because the track foundation stiffness varies dramatically under the impact force.

CONTENTS

1. Introduction

Wheel and rail running surfaces are not perfectly smooth but contain discontinuities, such as rail joints, switches and wheel flats. Flats are formed on a railway wheel by locking of the wheel during braking and may be typically 50 mm long, extending to over 100 mm long. The geometry of a rail joint can be characterized by the gap width and the height difference in the two sides of a gap. The gap width may be typically 5-20 mm and the height difference 0.5-2 mm. These discontinuities on the wheel and rail can generate large impact forces between the wheel and track when wheels with flats subsequently rotate or wheels roll over a rail joint. As a consequence, a transient impact noise is produced in addition to the usual rolling noise, which is more stationary in character.

Wheel/track impact has been studied over many years. A detailed study of the interaction between a wheel and the track in response to wheel flats was carried out by Newton and Clark [1], including both prediction and measurement aspects. The track model used in [1] is linear and consists of an infinite beam, representing the rail, on an elastic foundation. Wu and Thompson [2, 3] studied wheel/rail impact due to wheel flats and rail joints using a simplified track model, which is represented by low order ordinary differential equations transformed from the frequency response function of the track. A finite element (FE) track model was used by Nielsen and Igeland [4] to study bogie/track interactions due to rail corrugation, wheel flats and unsupported sleepers and by Andersson and Dahlberg [5] to investigate wheel/rail impact due to a wheel or bogie passing over a railway turnout crossing. In the above studies all track models were assumed to be linear, although the wheel/rail interface was considered as non-linear and described by a Hertzian contact spring.

In a railway track, the rails are supported by pads, sleepers and ballast. Although the pads and ballast are non-linear, they are usually assumed to be linear in order to simplify the track model. This may cause incorrect results to some extent in some circumstances, as the pad and ballast stiffness varies with loads. Moreover, adjacent sleepers may be lifted clear of the ballast under axle loads as ballast cannot sustain tensions. A non-linear track model is therefore needed to take account of these properties and their effects on wheel/track dynamics. Dong et al [6] studied wheel/rail impact due to wheel flats using an FE track model, in which

loss of contact between the rail and rail pads and between the sleepers and ballast was taken into account, although the pads and ballast were assumed to be linear. Wu and Thompson [7, 8] investigated the effects on track dynamics of the non-linearity of the pad and ballast using an equivalent linear track model, in which the stiffness of each track support was determined using a non-linear static track model. It was shown that only a few supports near the wheel loads were stiffened, and at those more than about 2 m away from the wheel the preloads in the pads and ballast due to vehicle weight were very low and thus negligible. Dahlberg [9] studied the rail deflection using a non-linear track model during the passage of a high-speed train bogie. It was found that the differences in the results between the non-linear and linear models were considerable. The results from [9] imply that if the load to the rail pad and ballast varies significantly, a non-linear track model is needed to simulate wheel/track dynamics. This is because the pad and ballast stiffness varies dramatically when the load in the pad and ballast varies significantly. In such cases a linear track model is not appropriate, for example, to calculate the rail deflection during a train passage as in [9], or to simulate wheel/track impact due to wheel and rail discontinuities.

The main objective of this study is to explore the effects on wheel/track impact of the non-linearity of the railway track supports. Wheel/track impacts are studied using a non-linear track model. In the model both the non-linear stiffness of the pad and ballast and potential loss of contact between the rail and rail pads and between the sleepers and ballast are taken into account. The rail is represented by an FE model using Timoshenko beam elements and interacts with the wheel through a non-linear Hertzian contact spring. Wheel/track impacts are simulated at different train speeds. Three types of rail pad, soft, medium and stiff, are used in the simulations. The results of wheel/track impact are presented in terms of the impact forces between the wheel and rail and in the pad and ballast, dynamic displacements of the wheel, rail and sleeper and the general vibration level of the rail and sleepers. These results are then compared with those from an equivalent linear track model to examine the effects of the track non-linearity. It is found that linear track models are not appropriate for wheel/track impact calculations because the differences in the results between the linear and non-linear track models are not ignorable.

2. Track non-linearity

Fig. 1 shows schematically the wheel/track interaction model. The vehicle system is simplified to a static load W and a wheel (unsprung mass M_w). This is because the vibration frequency of interest here is within the audio frequency range, for example 50-2000 Hz, whilst the natural frequency of the vehicle-suspension system is only a few Hertz, and thus the low frequency vibration of the vehicle body and bogie is effectively isolated from the high frequency vibration of the wheel and track. At frequencies above about 1.5 kHz wheel resonances should be taken into account but for simplicity these are omitted here. The track model is composed of a Timoshenko beam on a discrete spring-mass-spring foundation representing the rail pad, sleeper and ballast respectively. The wheel and rail interact via a Hertzian contact stiffness which is non-linear; the contact force is proportional to the elastic contact deflection to the power 3/2 provided loss of contact does not occur.

For simplicity the pad and ballast stiffness is usually assumed to be linear and no loss of contact is allowed between the rail and pad and between the sleeper and ballast in the track dynamics. Damping can be introduced by adding loss factors to the pad and ballast stiffness. In practice, however, the pad and ballast stiffness is non-linear and increases with the preloads in them. Fig. 2(a) shows the measured static stiffness of two types of pad [10]. The static stiffness can be seen to increase with the load. For the medium pad measured, the stiffness increases with load linearly. For the stiff pad measured, the stiffness increases dramatically with load up to about 20 kN, and beyond 20 kN it still increases, although more gently. According to the measured results, the pad stiffness k_p can be assumed to increase with load linearly or piece-wise linearly, such as

$$k_p = k_0 + bf_p, \tag{1}$$

where k_0 is the pad stiffness without load, f_p is the load to the pad and b is the rate of increase.

The pad dynamic stiffness at high frequencies is generally higher than the static stiffness due to the non-linear properties of the elastomers, and at sufficiently high frequency due to internal resonances. The pad dynamic stiffness has been measured by Thompson et al [11] using an indirect method and a specifically designed test rig. Their results showed that the pad dynamic stiffness varies with preload and frequency, for example, for a Pandrol studded 10

mm pad, its dynamic/static stiffness ratio changes from 3.5 to 4.5 under a 40 kN preload when the frequency increases from 50 to 500 Hz, and the ratio varies between 3.5-3.8, as the preload varies between 20 and 80 kN at 200 Hz. The ballast stiffness also varies with preload and frequency [12]. In a wheel/track interaction model the dynamic stiffness of the railway track should be used rather than the static stiffness. The pad dynamic stiffness used in this study is shown in Fig. 2(b). For the medium pad the dynamic/static stiffness ratio is chosen to be 3.6 and for the stiff pad it is chosen to be 2.3 [10]. For simplicity the relation between the preload and stiffness is approximated to be linear as shown in Figs. 2(a) and 2(b). The dynamic stiffness for the soft pad and for the ballast used here are from the measurements by Dahlberg [9], and they are represented approximately by

$$k_p = 52 + 6.24\times10^8 x_p^2 \ \text{MN/m}, \tag{2}$$

$$k_b = 22.75 + 2.60\times10^8 x_b^2 \ \text{MN/m}, \tag{3}$$

where k_p and k_b are the soft pad and ballast stiffness respectively, and x_p and x_b are the compression (in metre) of the pad and ballast respectively.

Since the stiffness of the medium and stiff pads is assumed to increase linearly with the load as shown in Eq. (1), and the tangent stiffness is given by $k_p = df_p / dx_p$, the stiffness-deflection and load-deflection laws can be derived as

$$k_p = k_0 e^{bx_p} \tag{4}$$

$$f_p = \frac{k_0}{b}(e^{bx_p} - 1). \tag{5}$$

For the dynamic stiffness of the medium pad k_0 = 115.2 MN/m and b = 7.49 mm^{-1}, while for the stiff pad k_0 = 1000.5 MN/m and b = 9.89 mm^{-1}. They are shown in Figs. 2(c) and 2(d). For the soft pad and ballast, the load-deflection laws can be derived from Eqs. (2) and (3) as

$$f_p = 52x_p + 2.08\times10^8 x_p^3 \ \text{MN}, \tag{6}$$

$$f_b = 22.75x_b + 0.87\times10^8 x_p^3 \ \text{MN}. \tag{7}$$

Apart from the non-linear load-deflection laws for the pad and ballast, another non-linearity of the railway track is that loss of contact may occur between the rail and rail pads and between the sleepers and ballast. This is also taken into account in the non-linear track model

in this study.

The track deformation and the preload in the track foundation caused by a 100 kN point force representing a static wheel load are calculated using a finite element model. Timoshenko beam elements [13] (see appendix) are used for the rail. Twenty sleeper bays are considered in the FE model, and the point force is applied in the middle of this length and above a sleeper. The length of a sleeper bay is chosen to be 0.6 m. Each piece of rail within a sleeper bay is divided into four Timoshenko beam elements. Natural boundary conditions are used at the two ends of the track, where the shear force and bending moment vanish. Since the track foundation is non-linear and the stiffness matrix of the track is load/deformation dependent, the point force applied to the track is divided into 100 increments and the calculations are performed in 100 steps. In each step the stiffness matrix is assumed to be constant and it is determined using the deformation from the previous calculation step. Although the force applied to the track is static, the dynamic stiffness of the pad and ballast is used in the calculations. In addition a 20 kN force is applied between the rail and sleeper at each support. This force is actually from the rail fasteners. Moreover, the weights of the rail and sleeper are also applied to the track. The rail weight is 0.6 kN per metre and each sleeper (half) weight is 1.6 kN.

Figs. 3 and 4 show the results for the railway tracks with soft and stiff pads respectively in terms of the track deformation at the forcing point and the loads in the pad and ballast. It can be seen that the track deformation caused by the point force occurs only in the near field of the wheel load. The foundation is therefore preloaded by the wheel load only within 3-4 sleeper bays on each side of the load. At a distance more than four sleeper bays away from the load, the preload in the foundation caused by the wheel load can be neglected. Compared with the track using soft pads, the deflection of the track using stiff pads is smaller and the preload is larger in the foundation close to the wheel load. Also shown in Figs. 3 and 4 are the pad and ballast stiffness. It can be seen that, due to the preload and non-linearity, the pad and ballast stiffness increase dramatically in the foundation near the wheel load. It is therefore expected that the impact force between the wheel and rail will increase due to the stiffening pad and ballast under the wheel load.

3. Wheel/track non-linear interaction models

A relative displacement excitation model is used to calculate wheel/track impact [14]. In such a model the wheel remains stationary on the rail and the discontinuities on the wheel and rail rolling surfaces are effectively moved at the train speed between the wheel and rail as an excitation [2, 3]. The wheel/track interaction model is shown schematically in Fig. 1. In this model the wheel interacts with the rail through a non-linear Hertzian contact spring and loss of contact between the wheel and rail is allowed. The equation of motion for the wheel is given as

$$\ddot{x}_w = \frac{1}{M_w}(W - f_c), \tag{8}$$

$$f_c = \begin{cases} C_H (x_w - x_r - r)^{3/2}, & x_w - x_r - r > 0 \\ 0, & x_w - x_r - r \le 0 \end{cases}, \tag{9}$$

where x_w is the wheel displacement, x_r is the rail displacement at the wheel/rail contact point, r is the moving discontinuity excitation due to the wheel flat or rail joint, M_w is the wheel mass (unsprung mass) and M_w = 600 kg, W is the vehicle load and W = 100 kN, f_c is the contact force and C_H is the Hertzian constant, taken here as $C_H = 93.7$ GN/m$^{3/2}$.

The rail is modelled using the finite element method and Timoshenko beam elements are used to represent the rail. The mass and stiffness matrices of the Timoshenko beam element are given in appendix. 40 sleeper bays (24 m long) are included, and each piece of rail in a sleeper bay is divided into four elements. The wheel/track impact is assumed to occur in the middle of the track. Natural boundary conditions are again used at the two ends of the track, where the shear force and bending moment vanish. The equation of motion for the rail is given by

$$\mathbf{M}_r \ddot{\mathbf{X}}_r + \mathbf{K}_r \mathbf{X}_r = \mathbf{F}_{sr} + \mathbf{F}_c + \mathbf{F}_p, \tag{10}$$

where $\mathbf{M}_r$ and $\mathbf{K}_r$ are the mass and stiffness matrices of the FE rail model respectively and $\mathbf{X}_r$ is the rail displacement vector. The forces applied to the rail consist of three components; $\mathbf{F}_{sr}$ is the static load vector including the rail weight and the clip forces on the rail side from the rail fasteners, $\mathbf{F}_c$ is the wheel/rail contact force presented in the vector form and $\mathbf{F}_p$ contains the forces due to the pad deflection and damping. $\mathbf{F}_p$ is non-linear and its elastic component

can be calculated using Eq. (5) or (6). When loss of contact occurs between the rail and pad, the pad deformation is zero and the corresponding element of $\mathbf{F_p}$ vanishes.

The equation of motion for the sleepers is given as

$$\mathbf{M_s}\ddot{\mathbf{x}}_s = \mathbf{F_{ss}} - \mathbf{F_p} + \mathbf{F_b}, \tag{11}$$

where $\mathbf{M_s}$ and $\mathbf{X_s}$ are the mass matrix and the displacement vector of the sleepers respectively, $\mathbf{F_{ss}}$ is the static load vector applied to the sleepers including the weight of the sleepers and the forces from the rail fastener on the sleeper side, and $\mathbf{F_b}$ contains the forces due to the ballast deformation and damping. $\mathbf{F_b}$ is non-linear and its elastic component can be calculated using Eq. (7). $\mathbf{F_b}$ vanishes when loss of contact occurs between the sleeper and ballast.

The damping in the pad and ballast is assumed to be viscous, as the track model is non-linear and the calculations should be performed in the time domain. Thus the hysteretic damping in the frequency domain needs to be transformed into the viscous damping in the time domain. The following formula is used to calculate the equivalent viscous damping from the hysteretic damping loss factor:

$$c_i = \eta_i m_i \omega_i, \tag{12}$$

where c_i is the equivalent viscous damping coefficient, η_i is the loss factor of the hysteretic damping of the pad and ballast, m_i is the equivalent mass and ω_i is the natural frequency. $i = 1$ and 2 are for the ballast and pad damping respectively. The loss factors for the ballast and pad are chosen to be $\eta_1 = 1$ and $\eta_2 = 0.25$ respectively.

Based on the fact that the rail vibrates on the ballast stiffness at the first order natural frequency [15], the equivalent mass and the first order natural frequency in Eq. (12) can be calculated approximately using formulae

$$m_1 = m_s + m_r \tag{13}$$

and

$$\omega_1 = \sqrt{k_b / m_1} \tag{14}$$

respectively, where m_s is the sleeper mass, $m_s = 162$ kg, m_r is the rail mass in a sleeper bay, $m_r = 36$ kg, and k_b is the ballast stiffness calculated by Eq. (3). Similarly, as the rail bounces on the pad stiffness at the second natural frequency of the track vibration, the equivalent mass

and the second order natural frequency in Eq. (12) can be calculated approximately using formulae

$$m_2 = \frac{m_s m_r}{m_s + m_r} \tag{15}$$

and

$$\omega_2 = \sqrt{k_p / m_2} \tag{16}$$

respectively, where k_p is the pad stiffness calculated using Eq. (2) or (4). As the equivalent viscous damping depends upon the pad and ballast stiffness, the damping coefficients c_1 and c_2 also are non-linear.

4. Wheel/track impact simulations

Numerical simulations are carried out using the models introduced in section 3 for the wheel/track non-linear impact due to the discontinuity on the wheel and rail rolling surfaces. Wheel/track impact may be caused by severe roughness or wheel and rail discontinuities such as rail joints, crossings or wheel flats. Here, only a wheel flat is considered. Impact due to a wheel flat can be studied alternatively by considering a round wheel rolling over a rail with a corresponding indentation on the rail head, for details see [1-3]. The following irregularity (indentation) on the railhead is used in the present simulations to represent a wheel flat [1]:

$$r = \frac{d}{2}(1 - \cos 2\pi \frac{z}{l}), \qquad 0 \le z \le l \tag{17}$$

where d = 1 mm is the wheel flat depth, l = 100 mm is the flat length. Taking V as the train speed, then $z = Vt$ and r forms the moving irregularity excitation between the wheel and rail.

The rail parameters used for the simulations are from UIC 60 rail, and they are:

$E = 2.1\times10^{11}$ N/m^2, $G = 0.77\times10^{11}$ N/m^2, $\rho = 7850$ kg/m^3,

$A = 7.69\times10^{-3}$ m^2, $I = 30.55\times10^{-6}$ m^4, $\kappa = 0.4$,

where E is the Young's modulus, G the shear modulus, ρ the density, A the cross-sectional area, I the second moment of area and κ the shear coefficient.

The equations of motion for the wheel, rail and sleepers are assembled to form a state-space model. A fourth order Runge-Kutta method is used to simulate the wheel/track non-linear impact. The simulation results are given in terms of the maximum impact forces between the

wheel and rail and in the track supports, and the general vibration level of the rail and sleepers. The rail vibration level is calculated using the following formula:

$$VL_r = \sum_{n=1}^{4N} \int_0^T v_m^2(t)dt, \tag{18}$$

where v_m is the vertical vibration velocity of the rail at each node, N is half the number of the sleeper bays (N = 20) in the track model (there are 4 nodes per sleeper bay), as the wheel/track impact is assumed to occur in the middle of the track and the rail vibration is symmetrical. T is the impact integration period and is chosen to be 0.06 seconds, which is long enough to capture the main impact event for all speeds considered. The vibration level of the sleepers during impact is calculated by

$$VL_s = \sum_{n=1}^{N} \int_0^T v_{sn}^2(t)dt, \tag{19}$$

where v_{sn} is the sleeper vibration velocity. The vibration level described by Eqs. (18) and (19) is proportional to the vibration energy of the track and is related to the impact noise generation.

Fig. 5 shows the results of impact for the tracks with soft, medium and stiff pads in the speed region 20-240 km/h. The impact is assumed to occur above a sleeper. The maximum impact forces can be seen to increase with running speed until they reach the peaks around 80-130 km/h for the different pads, then decrease with running speed, although the wheel/rail impact force still keeps increasing after 130 km/h for the soft pad track. It is also observed that the impact forces are large when the stiff pads are used, for example, the maximum/static wheel/track force ratio can be as high as up to 8 in this case. Thus, using soft pads can reduce impact forces significantly. It can be seen from Fig. 5 that the impact force is the largest between the wheel and rail and is the smallest in the ballast because of the inertia of the rail and sleeper, the distributing effect of the rail and the isolation provided by the pad. On the other hand, the rail vibration level is the highest and the sleeper vibration level is the lowest when the soft pads are used. For the latter it is because the impact forces transmitted to the sleepers are the lowest among the three types of rail pad.

For comparison, the wheel/track impacts are also calculated using a linear track model, in which the support stiffness is assumed to be constant, although the pad and ballast stiffness is

different at the different positions. These are chosen to be the non-linear stiffnesses under a 100 kN static preload calculated in section 2 using the non-linear track model, see Figs. 3 and 4 for example. In addition, there is no loss of contact allowed between the rail and rail pads and between the sleepers and ballast, although the wheel/rail loss of contact is considered in the model. The results calculated using the linear track model are shown in Fig. 6. It can be seen that the maximum impact forces from the linear model are much smaller, compared with those from the non-linear track model, especially for the tracks using the stiff and medium pads. This is because the non-linear stiffness of the pad and ballast increases with the load. Under a high load the pad and ballast become very stiff, as a result of which the impact force is very high. The vibration level of the linear track is mostly lower than that of the non-linear track. The reason for this is that the calculated displacement is larger when a non-linear track model is used, as the deformation in the track foundation is relatively larger at the early loading stage due to the soft stiffness under a small load of the non-linear pad and ballast, and therefore the final displacement and velocity of the non-linear track are larger. In addition the impact forces from the linear track are lower, and so they result in lower level vibration responses.

Comparing the results from the non-linear track model with those from the linear model, it can be concluded that for wheel/track impact problems a linear track model is not appropriate because the impact load is very large and the pad and ballast stiffnesses increase dramatically with the load. Moreover, large impact forces often result in loss of contact between the sleepers and ballast, and this is not allowed by a linear model. However, if the excitation is the roughness on the wheel and rail rolling surfaces, a linear track model can be used, as in this case the wheel/rail interaction force is moderate [16].

The wheel/track impact is also simulated for the impact occurring at mid-span. The results are shown in Figs. 7 and 8 for the non-linear and linear track models respectively. The variation of the impact forces and vibration level with the speed and pad type and the differences in the results between the non-linear and linear models are similar to those for the impact occurring at a sleeper, although the dependence of the wheel/rail impact forces with the running speed are shown to be more complicated. The impact forces at the pad and ballast are smaller here because the support where the impact forces are shown is half a sleeper bay

away from the wheel.

More detailed information and characteristics of the non-linear wheel/track impact can be observed from the time series of the impact forces and displacements. Figs. 9 and 10 show the wheel/rail impact force, the impact forces in the supports and the displacements of the wheel, rail and sleeper at the impact position due to a wheel flat used in the previous simulations. The simulation results in Figs. 9 and 10 are from the tracks with the soft and stiff pads respectively for a running speed of 120 km/h and for the wheel above a sleeper when the impact occurs. At this speed the maximum wheel/track impact force is locally minimum for the soft pad track, see Fig. 5, but for the stiff pad track it is near to the local maximum.

When the indentation (relative displacement input due to the wheel flat) appears between the wheel and rail (the sign convention adopted is positive for an indentation and for downwards displacements), the wheel falls and the rail rises. Since the wheel and rail cannot immediately follow the indentation due to their inertia, the contact force is therefore unloaded and loss of contact occurs between the wheel and rail. When the wheel contacts the rail again, impact occurs and the contact force increases rapidly until it reaches its peak. For the track with the soft pads the maximum wheel/track impact force is about 270 kN, whereas for the track with the stiff pads the impact force reaches a peak of 800 kN. Thus using soft rail pads can effectively reduce the impact forces. It can be seen from Figs. 9 and 10 that the impact forces in the pad are also high, although the impact forces in the sleeper are relatively lower. It can be observed that the high impact forces in the track foundation only appear at the nearest support to the wheel. At other supports the impact forces are dramatically reduced. Since the sleepers are attached to the rail, loss of contact occurs between the sleepers and ballast when the rail bounces during the impact. Moreover, loss of contact occurs between the rail and rail pads for the track with the stiff pads, even though 20 kN clip forces are applied. The small ripples in the wheel/rail and pad impact forces at a high frequency (about 1 kHz) are due to the vibration wave reflections from the rail ends, as the track model here is not infinitely long and thus the propagating waves in the rail cannot effectively decay to zero.

Fig. 11 shows the spectra of the wheel/track impact force and the impact forces in the pad and ballast at the first support corresponding to the results shown in Figs. 9 and 10. The spectra in Figs. 11(a) and 11(b) are for the track with the soft and stiff pads respectively. From

Fig. 11 the impact forces can be seen to show a broadband characteristic. The force spectra from the stiff pad track are shown to be slightly higher than those from the soft pad track at high frequencies because the impact is sharper for the stiff pad track.

5. Conclusions

Wheel/track impact has been studied using a non-linear foundation stiffness and allowing loss of contact between the track components in the track model. The rail is modelled using the FE method with Timoshenko beam elements. Wheel/track impact has been simulated using a relative displacement input at different train speeds. Three types of rail pad, soft, medium and stiff, have been used in the simulations.

The pad and ballast stiffness is effectively non-linear, load-dependent and it increases with the load. Due to the non-linearity of the track the foundation near the wheel load is stiffened, but only a few supports are influenced. The impact forces between the wheel and rail and in the track foundation increase with increasing pad stiffness. Impact forces rise dramatically when stiff rail pads are used. Thus using soft pads can reduce impact forces significantly. On the other hand, however, soft pads increase the rail vibration level and thus the impact noise radiation from the rail. Non-linearity of the railway track may also involve loss of contact between the rail and rail pads and between the sleepers and ballast. This occurs when the wheel/rail contact force is unloaded and the rail bounces during impact. Compared with the simulation results using the linear track model, both the impact forces and the track vibration level are shown to be noticeably higher from the non-linear track model than those from the linear track model. This can be justified from three aspects. First, under a high load the non-linear pad and ballast become very stiff; as a result the impact forces are very high. Second, the deformation of the non-linear foundation is relatively larger at the early loading stage due to its soft stiffness under a small load, and therefore the displacement and velocity are larger for the non-linear track. Finally, the lower impact forces from the linear track result in lower level vibration responses.

It can be concluded that linear track models are not wholly appropriate for wheel/track impact problems. However, if the excitation is due to roughness on the wheel and rail rolling

surfaces, linear track models can be used, as in this case the wheel/rail interaction force is moderate.

6. Acknowledgements

The work described has been supported by EPSRC (Engineering and Physical Sciences Research Council of the United Kingdom) under the project 'Non-linear Effects at the Wheel/rail Interface and their Influence on Noise Generation', grant GR/M82455. The modelling and simulation parts of the work were carried out while the first author was at ISVR.

References

[1] S. G. Newton, R. A. Clark, An investigation into the dynamic effects on the track of wheelflats on railway vehicles, Journal Mechanical Engineering Science 21 (1979) 287–297.

[2] T. X. Wu, D. J. Thompson, A hybrid model for the noise generation due to railway wheel flats, Journal of Sound and Vibration 251 (2002) 115-139.

[3] T. X. Wu, D. J. Thompson, On the impact noise generation due to a wheel passing over rail joints, Proceedings of the 7th International Workshop on Railway Noise, Portland, Maine, USA, 2001.

[4] J. C. O. Nielson, A. Igeland, Vertical dynamic interaction between train and track—influence of wheel and track imperfections, Journal of Sound and Vibration 187 (1995) 825-839.

[5] C. Andersson, T. Dahlberg, Wheel/rail impacts at a railway turnout crossing, Proceedings of the Institution of Mechanical Engineers, Part F, 212 (1998) 123-134.

[6] R. G. Dong, S. Sankar, R. V. Dukkipati, A finite element model of railway track and its application to the wheel flat problem, Proceedings of the Institution of Mechanical Engineers, Part F, 208 (1994) 61-72.

[7] T. X. Wu, D. J. Thompson, The effects of local preload on the foundation stiffness and vertical vibration, Journal of Sound and Vibration 219 (1999) 881-904.

[8] T. X. Wu, D. J. Thompson, The vibration behaviour of railway track at high frequencies

under multiple preloads and wheel interactions, J. Acoust. Soc. Am. 108 (2000) 1046-4053.

[9] T. Dahlberg, Dynamic interaction between train and non-linear railway track model, Proceedings of the 5th European Conference on Structural Dynamics, Munich, 2002 pp. 1155-1160.

[10] P. Bouvet, N. Vincent, Laboratory characterization of rail pad dynamic properties, Vibratec Report 450.004.RA.05.A, 1998.

[11] D. J. Thompson, W. J. Van Vliet, J. W. Verheij, Development of the indirect method for measuring the high frequency dynamic stiffness of resilient elements, Journal of Sound and Vibration 213 (1998) 169-188.

[12] N. Frémion, J. P. Goudard, N. Vincent, Improvement of ballast and sleeper description in TWINS—step 1: experimental characterisation of ballast properties, VIBRATEC Report 072.028a, 1996.

[13] M. Petyt, Introduction to finite element vibration analysis, Cambridge University Press, Cambridge 1990.

[14] S. L. Grassie, R. W. Gregory, D. Harrison, K. L. Johnson, The dynamic response of railway track to high frequency vertical excitation, Journal Mechanical Engineering Science 24 (1982) 77-90.

[15] T. X. Wu, D. J. Thompson, A double Timoshenko beam model for vertical vibration analysis of railway track at high frequencies, Journal of Sound and Vibration 224 (1999) 329-348.

[16] T. X. Wu, D. J. Thompson, Theoretical investigation of wheel/rail non-linear interaction due to roughness excitation, Vehicle System Dynamics 34 (2000) 261-282.

Appendix: finite element for Timoshenko beam

For beam vibration at high frequencies, the shear deformation and rotary inertia effects should be taken into account. Thus Timoshenko beam elements are used for the rail FE model in this study. The mass and stiffness matrices of a Timoshenko beam element are given as [13]

$$\mathbf{M}_e = \frac{\rho A a}{210(1+3\beta)^2}\begin{bmatrix} m_1 & & & \\ m_2 & m_5 & & \text{Sym} \\ m_3 & -m_4 & m_1 & \\ m_4 & m_6 & -m_2 & m_5 \end{bmatrix} + \frac{\rho I}{30a(1+3\beta)^2}\begin{bmatrix} m_7 & & & \\ m_8 & m_9 & & \text{Sym} \\ -m_7 & -m_8 & m_7 & \\ m_8 & m_{10} & -m_8 & m_9 \end{bmatrix} \tag{A1}$$

where ρ is the density, A the cross-sectional area, I the second moment of area, a half the length of the element,

$$\begin{aligned} m_1 &= 156+882\beta+1260\beta^2 \\ m_2 &= (44+231\beta+315\beta^2)a \\ m_3 &= 54+378\beta+630\beta^2 \\ m_4 &= (-26-189\beta-315\beta^2)a \\ m_5 &= (16+84\beta+126\beta^2)a^2 \\ m_6 &= (-12-84\beta-126\beta^2)a^2 \\ m_7 &= 18 \\ m_8 &= (3-45\beta)a \\ m_9 &= (8+30\beta+180\beta^2)a^2 \\ m_{10} &= (-2-30\beta+90\beta^2)a^2 \end{aligned} \tag{A2}$$

β is given by

$$\beta = \frac{EI}{\kappa A G a^2} \tag{A3}$$

where E is the Young's modulus, G the shear modulus and κ the shear coefficient, and

$$\mathbf{K}_e = \frac{EI}{2a^3(1+3\beta)}\begin{bmatrix} 3 & & & \\ 3a & (4+3\beta)a^2 & & \text{Sym} \\ -3 & -3a & 3 & \\ 3a & (2-3\beta)a^2 & -3a & (4+3\beta)a^2 \end{bmatrix} \tag{A4}$$

The corresponding nodal deflections are

$$\mathbf{X}_e = [\, w_1 \;\phi_1 \; w_2 \;\phi_2 \,]^T \tag{A5}$$

where w_i is the vertical deflection and ϕ_i is the rotation of the cross-section.

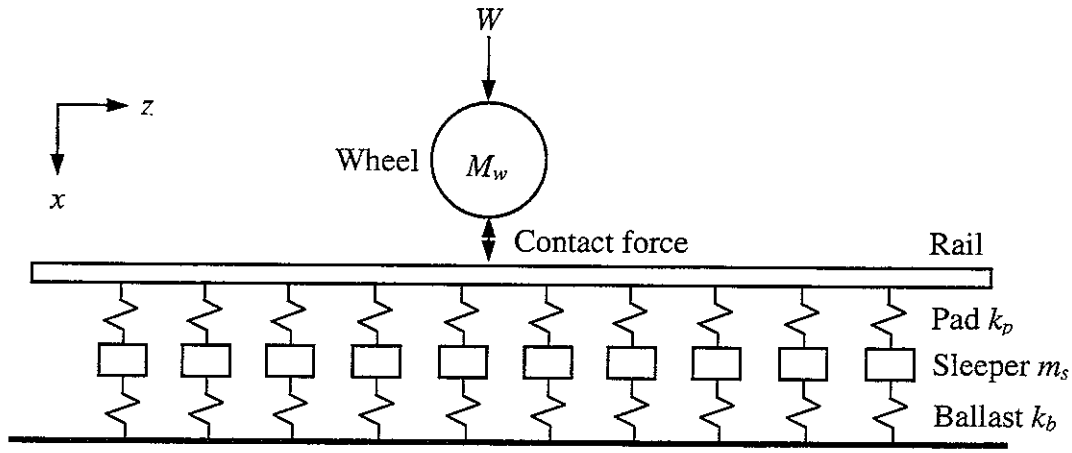

Fig. 1. Wheel/track interaction model.

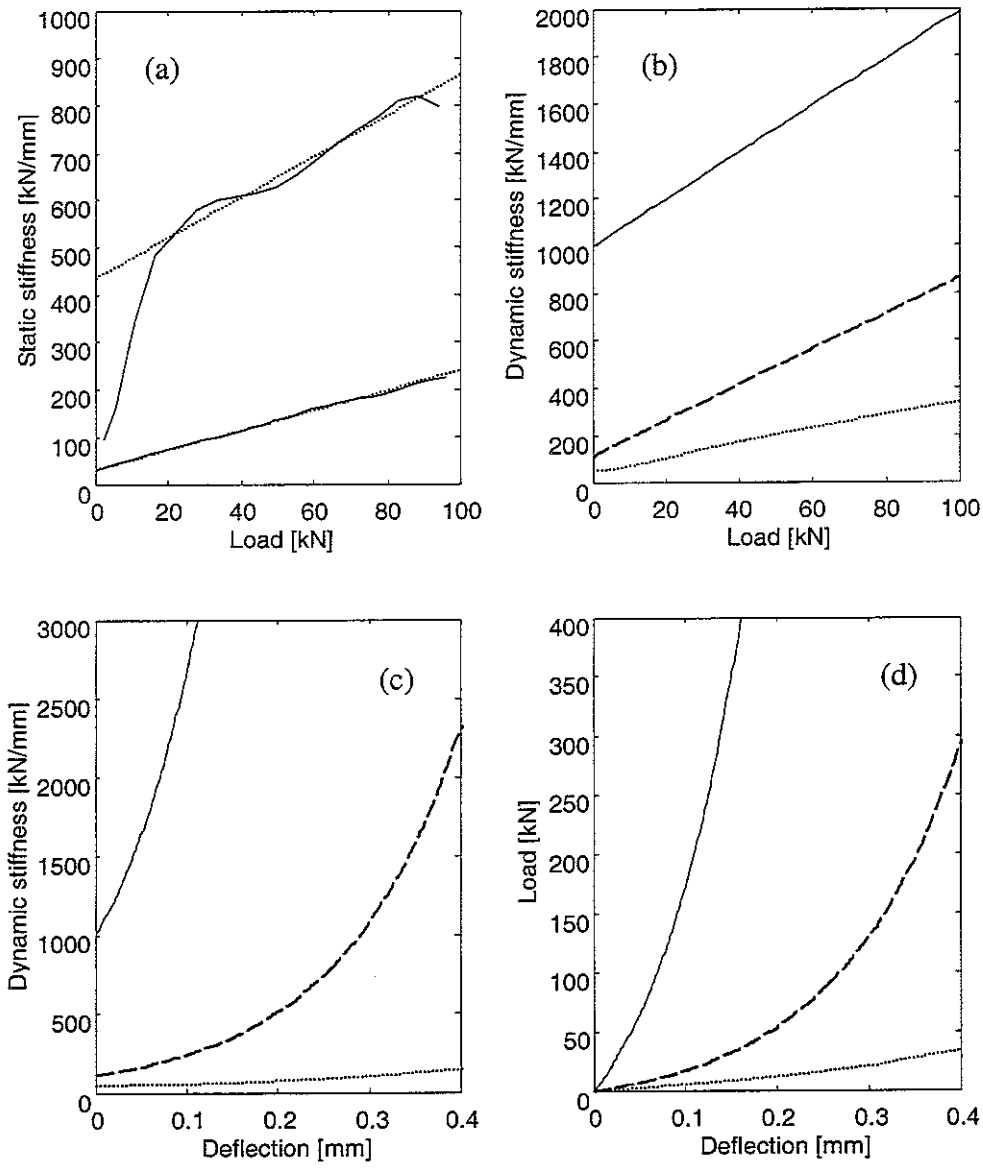

Fig. 2. (a) static stiffness of non-linear pads, — measured [10], ···· approximated. The upper curves are for the stiff pad and the lower curves are for the medium pad. (b) dynamic stiffness of non-linear pads, — stiff pad, --- medium pad, ···· soft pad. (c) and (d) stiffness-deflection and load-deflection laws for non-linear pads, — stiff pad, --- medium pad, ···· soft pad.

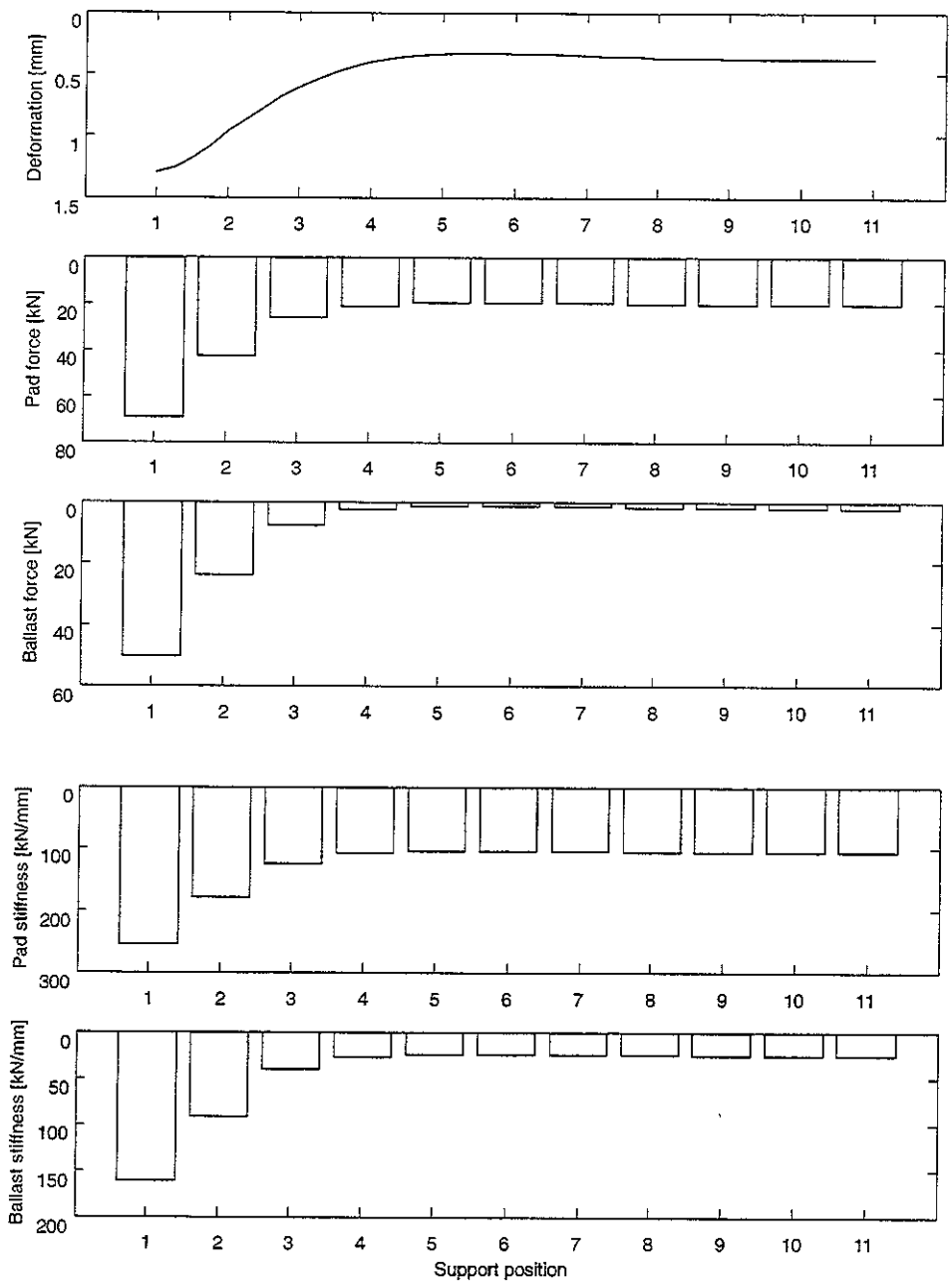

Fig. 3. Foundation deformation, preloads and dynamic stiffness of the pad and ballast of a non-linear railway track with soft pads under a 100 kN point force, clip forces and weights. The point force is applied to the rail above a sleeper.

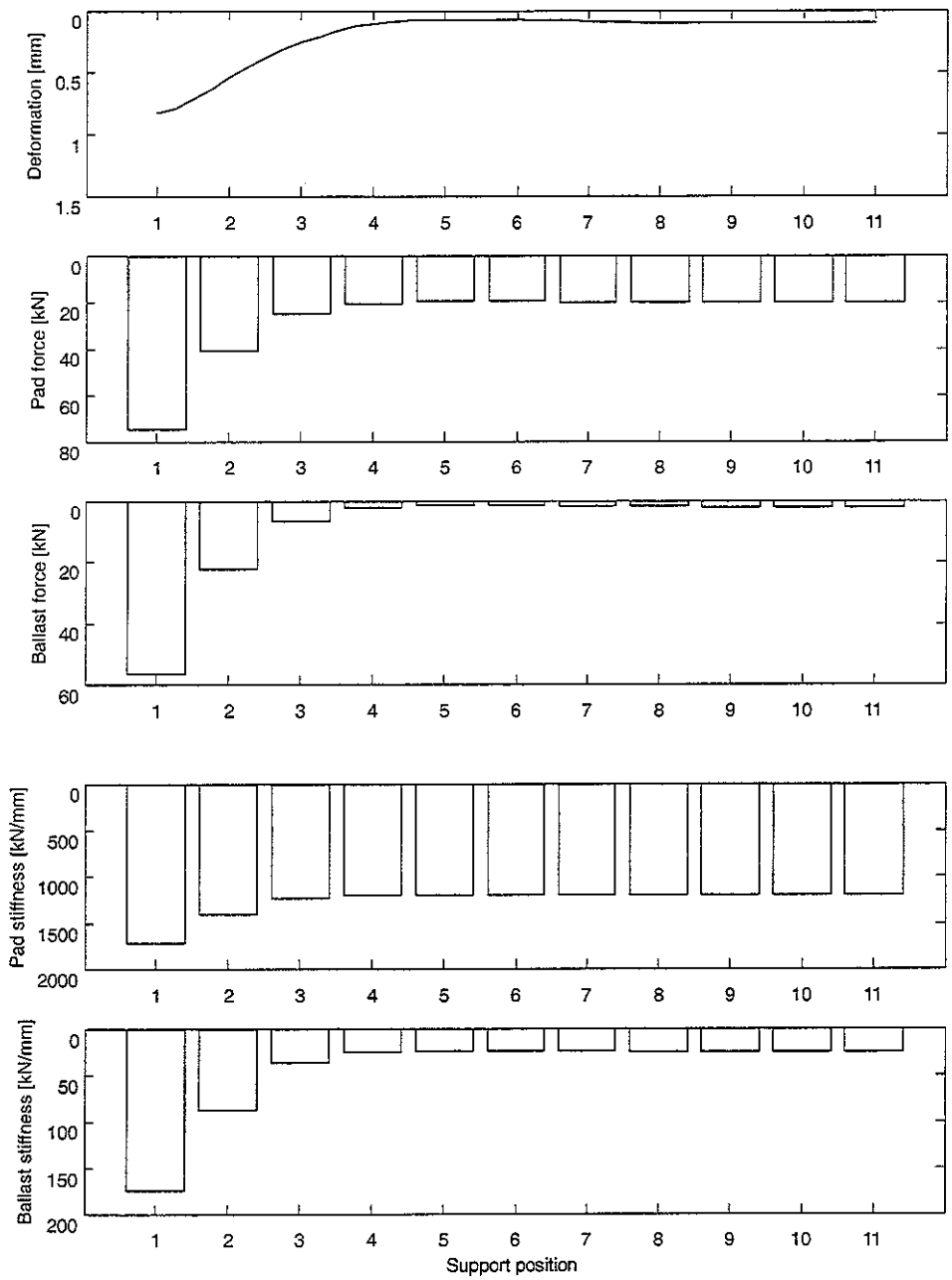

Fig. 4. Foundation deformation, preloads and dynamic stiffness of the pad and ballast of a non-linear railway track with stiff pads (as Fig. 3).

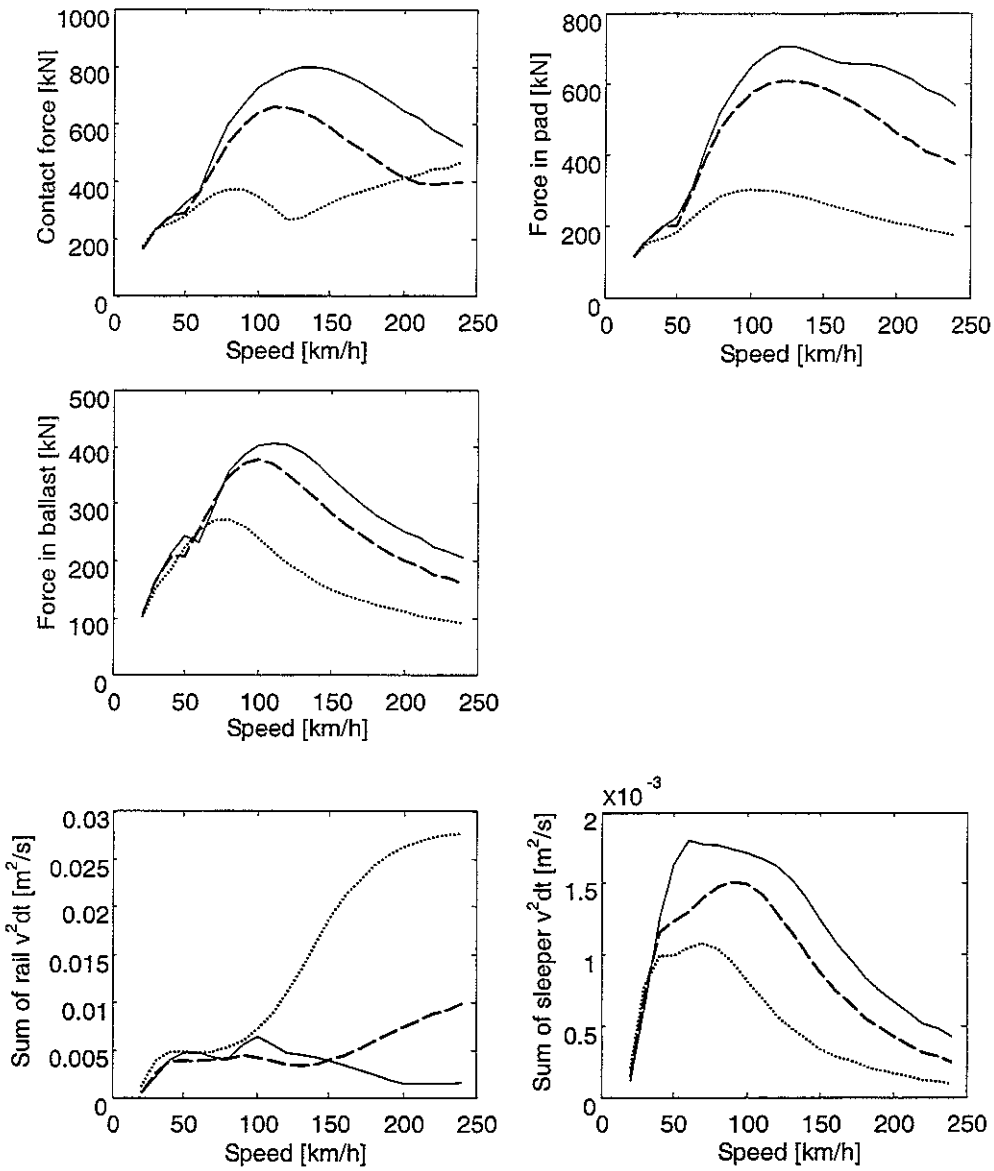

Fig. 5. Maximum impact forces and general vibration levels during impact (0.06 seconds) above a sleeper at different running speeds. The maximum forces in the pad and ballast are from the support where the wheel/track impact occurs. — for the track with stiff pads, --- medium pads, ···· soft pads.

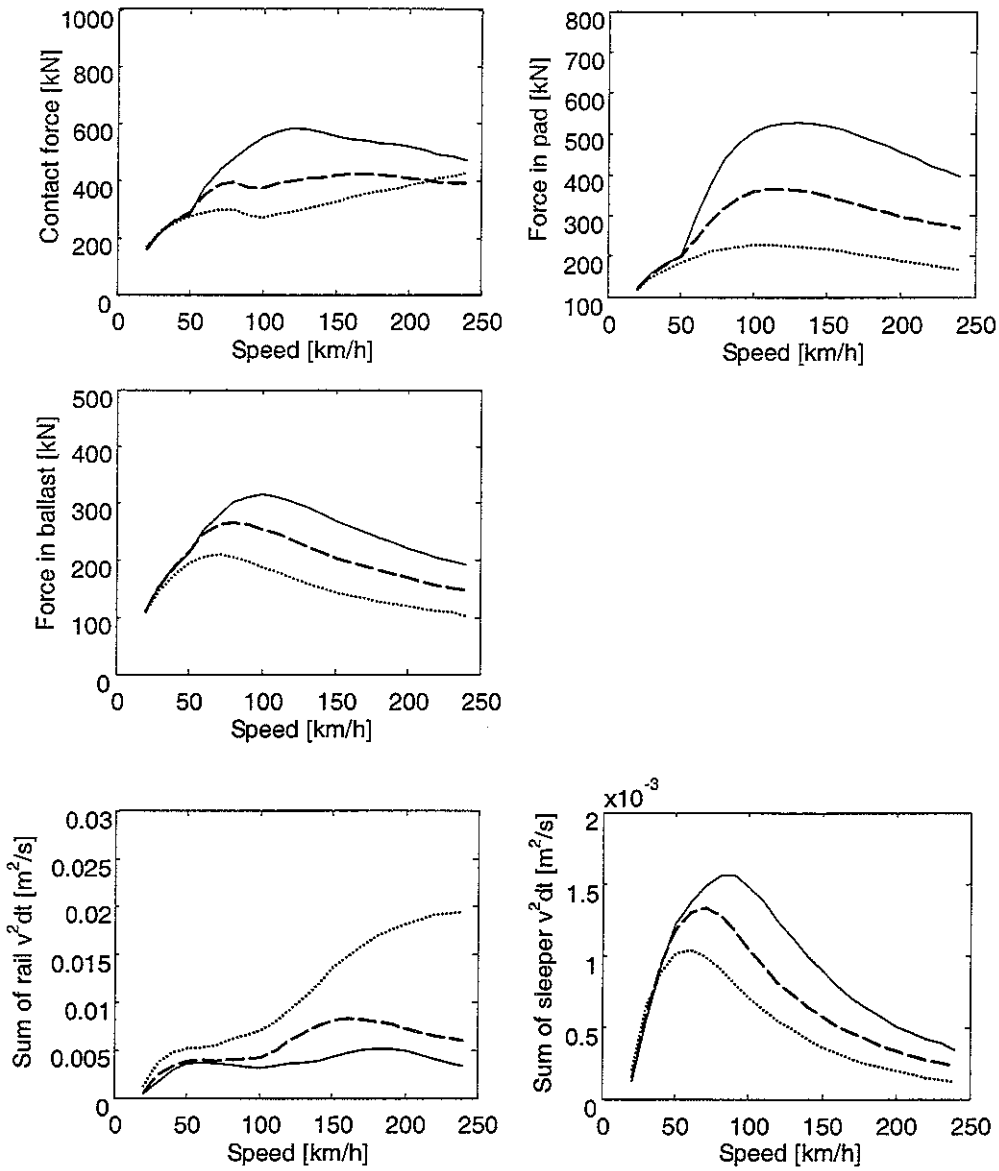

Fig. 6. Maximum impact forces and general vibration levels during impact at different running speeds, key as for Fig. 5, but the track model used is linear.

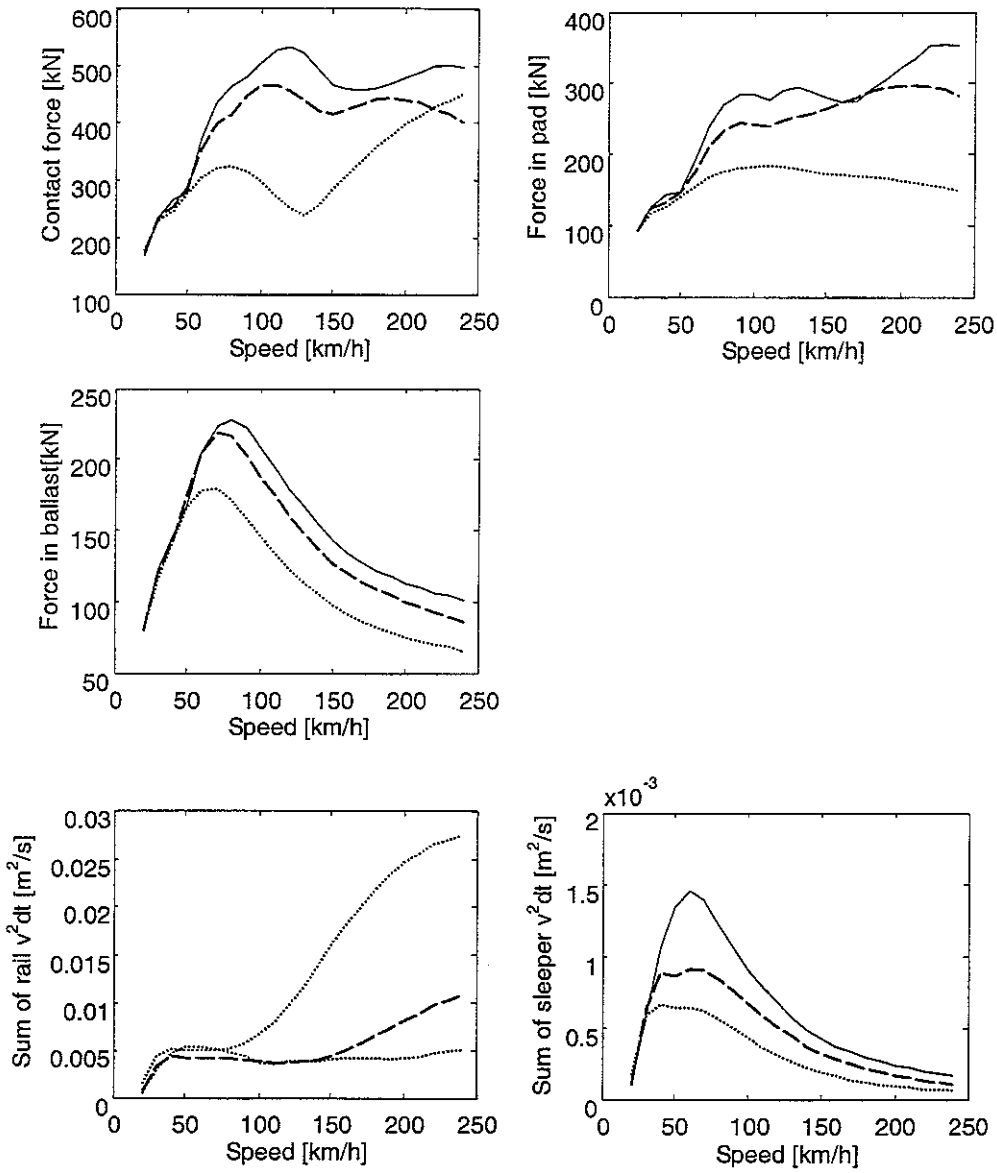

Fig. 7. Maximum impact forces and general vibration levels during impact at different running speeds, key as for Fig. 5, but wheel/track impact occurs at mid-span and the maximum impact forces in the pad and ballast are from the support nearest to the impact position.

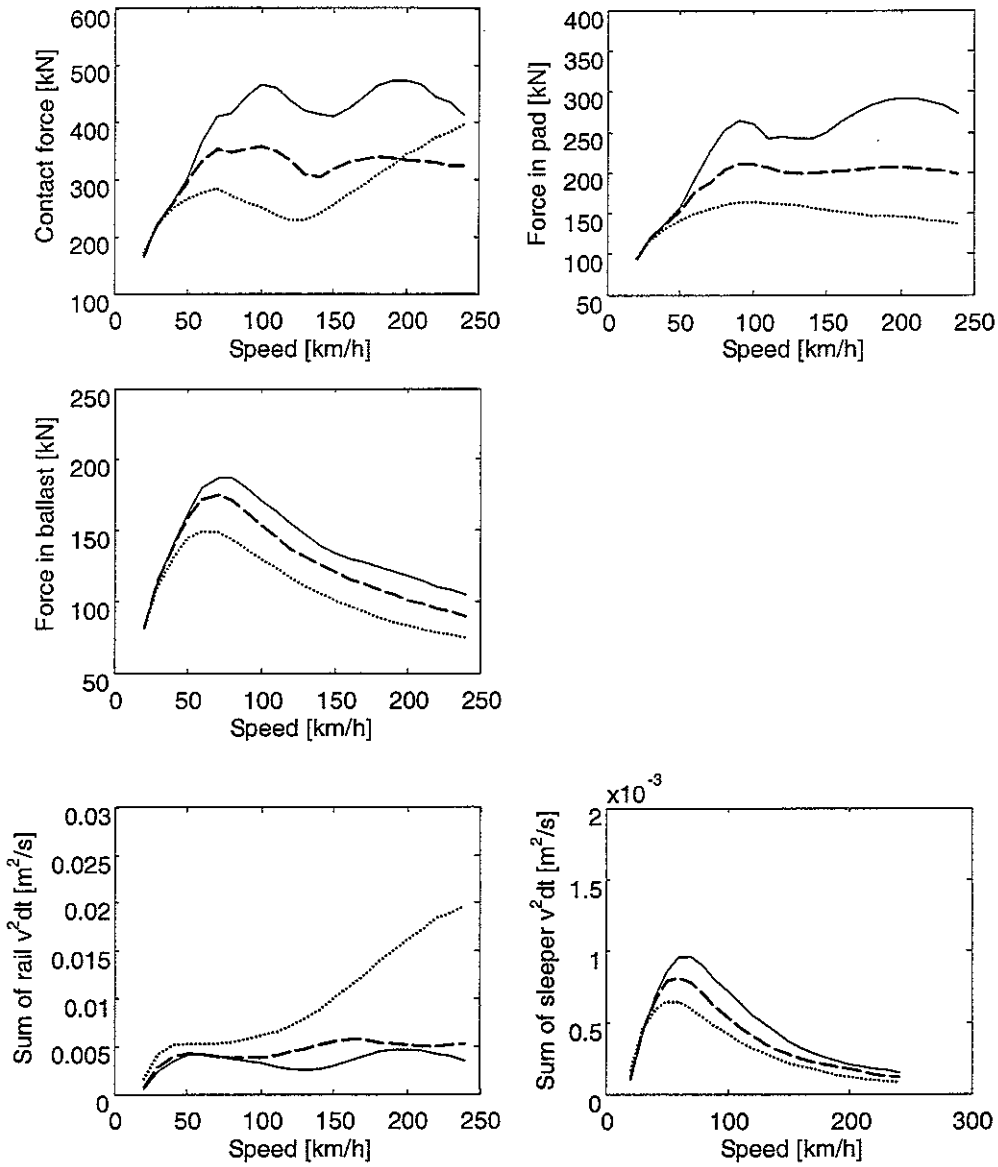

Fig. 8. Maximum impact forces and general vibration levels during impact at different running speeds, key as for Fig. 7, but the track model used is linear.

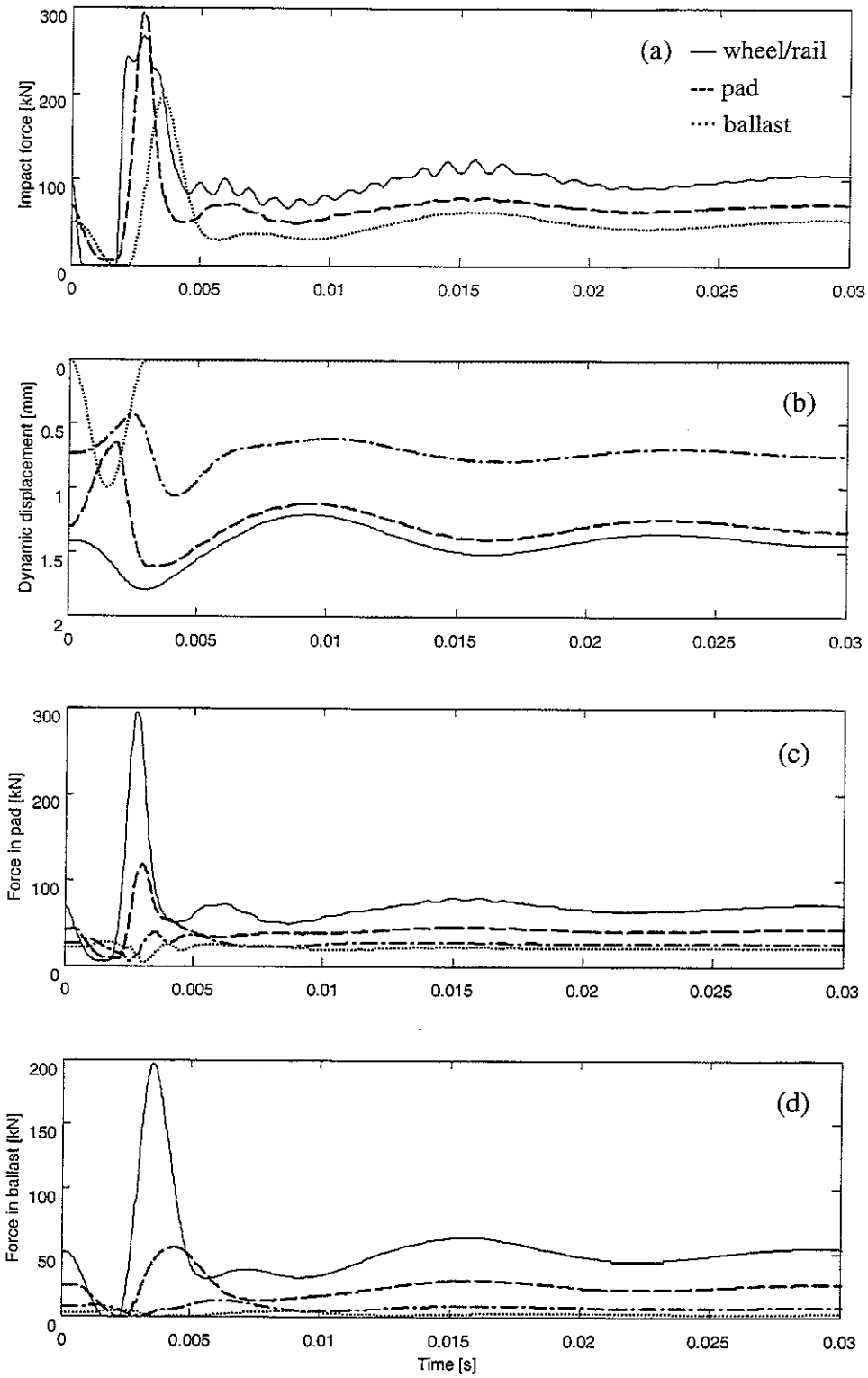

Fig. 9. Impact forces, displacements at the contact position of the wheel and track with soft pads. The running speed is 120 km/h and the impact occurs above a sleeper. The pad and ballast forces in (a) are from the 1st support where impact occurs. For (b) — wheel, --- rail, -·- sleeper, ···· relative displacement input; for (c) and (d) — at 1st support, --- 2nd support, -·- 3rd support, ···· 4th support.

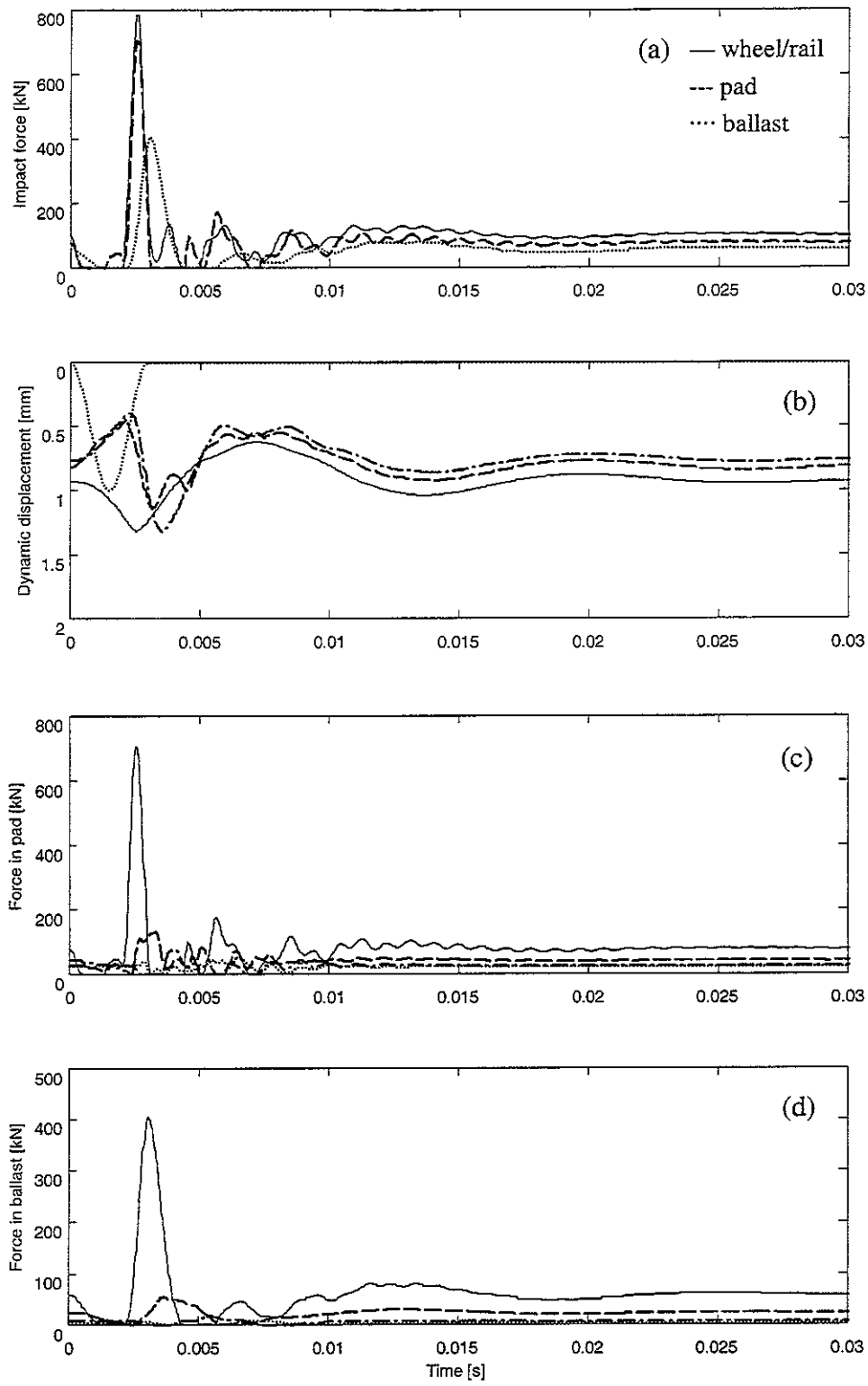

Fig. 10. Impact forces, displacements at the contact position of the wheel and track with stiff pads, key as for Fig. 9.

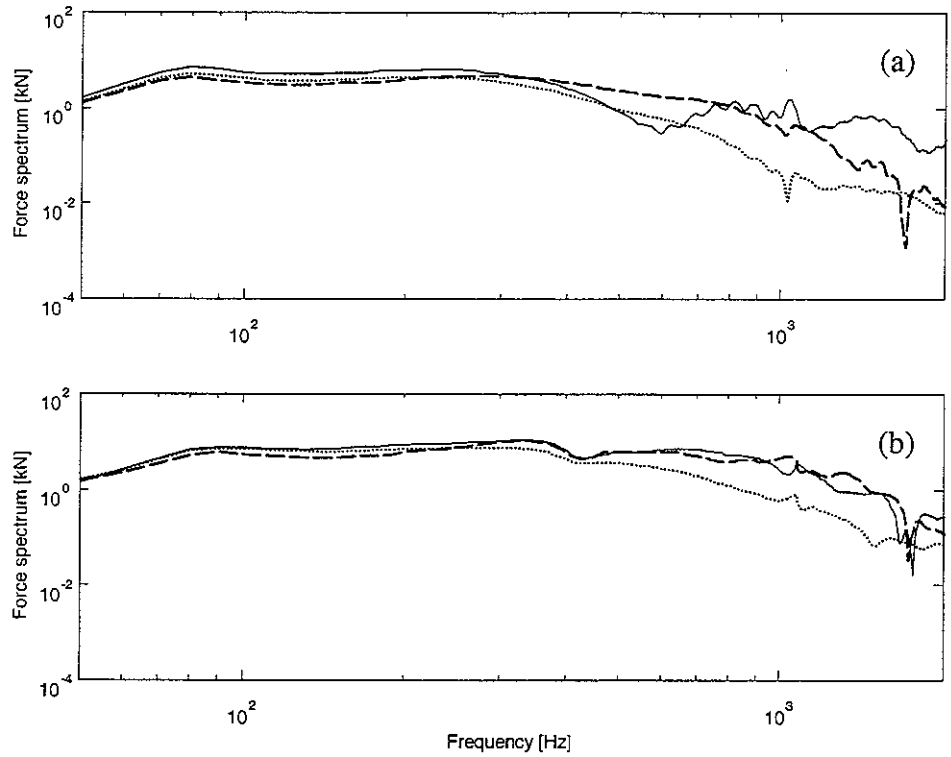

Fig. 11. Spectra of the wheel/track impact force and the impact forces in the track foundation at the nearest support to the impact. The running speed is 120 km/h and the impact occurs above a sleeper. (a) and (b) are for the track with the soft and stiff pads respectively. — wheel/rail impact force, --- force in pad, ···· force in ballast.